

# Planetary wave-tidal interactions over the equatorial mesosphere-lower thermosphere region and their possible implications for the equatorial electrojet

C. Vineeth,<sup>1</sup> T. K. Pant,<sup>1</sup> S. G. Sumod,<sup>1</sup> K. K. Kumar,<sup>1</sup> S. Gurubaran,<sup>2</sup> and R. Sridharan<sup>3</sup>

Received 1 July 2010; revised 18 October 2010; accepted 8 November 2010; published 27 January 2011.

[1] Optically measured daylight mean mesopause temperatures over a dip equatorial station, Trivandrum (8.5°N; 77°E; dip lat. 0.5°N), have been analyzed in conjunction with simultaneously measured equatorial electrojet (EEJ)-produced magnetic field at the surface. The signature of planetary wave-tidal interactions in the mesosphere-lower thermosphere (MLT) region has been observed for the first time in the day-to-day variability in the EEJ, i.e., the time of its peaking and the duration, as inferred from the EEJ-produced magnetic field on the ground. The present study shows that the planetary wave of quasi 16 day periodicity plays an important role in causing these variabilities, especially during the winter months. The quasi 16 day wave is found to be modulating the mesopause temperature (MT), duration, and time of the maximum EEJ intensity ( $D_{EEJ}$  and  $T_{EEJ}$ ). During positive excursions of the planetary wave,  $T_{EEJ}$  showed a shift toward evening, while the MT showed an increase and  $D_{EEJ}$  showed a broadening. Similarly, all these parameters exhibited an opposite trend during negative excursions. The planetary wave-tidal interactions and subsequent modification of the tidal components have been shown to be responsible for the observed variations. This study presents a new perspective addressing the day-to-day variability of the EEJ.

**Citation:** Vineeth, C., T. K. Pant, K. K. Kumar, S. G. Sumod, S. Gurubaran, and R. Sridharan (2011), Planetary wave-tidal interactions over the equatorial mesosphere-lower thermosphere region and their possible implications for the equatorial electrojet, *J. Geophys. Res.*, 116, A01314, doi:10.1029/2010JA015895.

## 1. Introduction

[2] The mesosphere-lower thermosphere (MLT) region, especially over the equatorial latitudes, is primarily driven by dynamical forcings. In the MLT region the mesosphere deserves special attention since it couples the lower atmosphere to the ionosphere above. The day-to-day variability in the temperature and wind fields in the mesosphere is thought to be governed primarily by dynamical forcings like the tides, planetary waves and gravity waves, which have sources mainly in the troposphere-stratosphere, and they grow in amplitude as they propagate upward. In the upper mesospheric region the impact of these dynamical forcings on the temperature, winds, and density structure is especially [Smith, 2004]. At equatorial latitudes atmospheric tides play a significant role in controlling both the neutral dynamics and the electrodynamics of the MLT region. The equatorial electrojet (EEJ), a unique geophysical phenomenon over the magnetic equator, is an outcome of the tidal diurnal wind-driven dynamo on a global scale [Fambitakoye and Mauyaud, 1976; Forbes, 1981].

[3] The observed variability in the EEJ current has been attributed to the electron density, conductivity and the tidal variabilities at EEJ heights [Richmond, 1973; Forbes, 1981; Reddy, 1981; Stening, 1985]. Among these, the upward propagating tides play a significant role in shaping the major phenomenology of the equatorial dynamo region on a day-to-day basis [Abdu *et al.*, 2006]. The strength of the EEJ exhibits great seasonal variability, being 1.7–1.8 times greater at equinoxes than at solstices [Reddy, 1989]. However, the day-to-day variability is mainly because of the variability in the tidal structure, which also exhibits large seasonal variability [Deepa *et al.*, 2006]. Tides have horizontal wind amplitudes that can exceed 50 m/s and temperature amplitudes of as much as 20 K at upper mesospheric altitudes [Hagan *et al.*, 1999]. Tidal amplitudes increase with altitude up to the lower thermosphere and vary somewhat regularly with season. The temperature perturbations associated with the tides are observed to be maximizing over the equator. Owing to the dominant tidal structures, the local time of maximum temperature varies with altitude, latitude, and season [Hagan *et al.*, 1999].

[4] Further, the tides may interact with planetary waves (PWs), which are also of lower atmospheric origin, causing variations in their amplitude and phase. These interactions are expected to be more effective in the mesosphere, as both PWs and tidal amplitudes are typically high in this region. In addition to this, the processes involving the PWs and their

<sup>1</sup>Space Physics Laboratory, Vikram Sarabhai Space Centre, Trivandrum, India.

<sup>2</sup>Equatorial Geophysical Research Laboratory, Tirunelveli, India.

<sup>3</sup>Physical Research Laboratory, Ahmedabad, India.

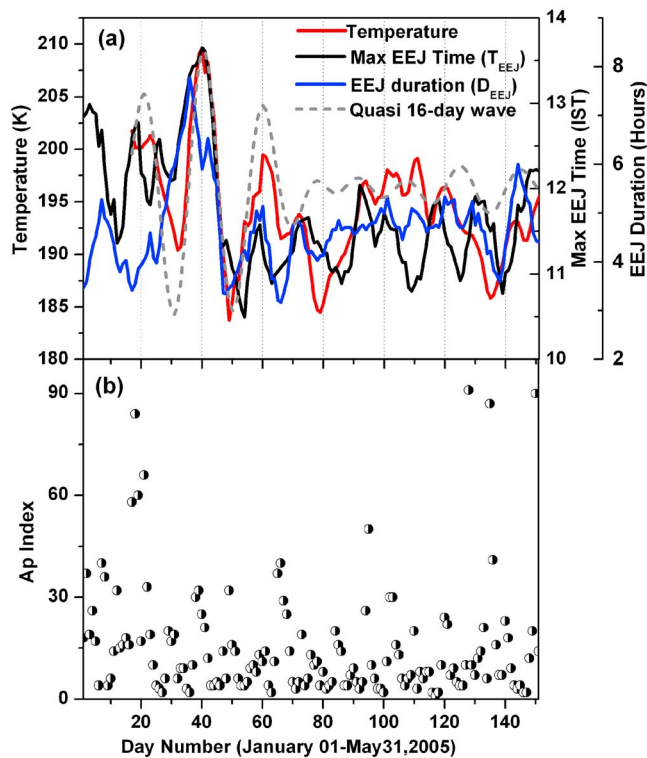


**Figure 1.** Time variation of daytime mesopause temperature (MT), time of the maximum equatorial electrojet (EEJ;  $T_{EEJ}$ ), and duration of the EEJ ( $D_{EEJ}$ ) over Trivandrum.

interaction with tides also are known to have a bearing on the day-to-day variabilities of the daytime equatorial electrodynamics, especially of the EEJ [Abdu *et al.*, 2006; Vineeth *et al.*, 2007]. The most prominent manifestations of this day-to-day variability of EEJ are the time at which the EEJ peaks: its strength and the duration. However, to understand and explain this variability, one needs to simultaneously investigate the daytime dynamics and energetics in the equatorial mesosphere and ionosphere regions.

[5] In this context, in recent years a unique dayglow photometer, along with a collocated meteor wind radar, has been providing systematic estimates of the daytime mesopause temperature and neutral wind, respectively, over Trivandrum (8.5°N, 77°E; dip latitude, 0.5°N), a dip equatorial station. These measurements, used in conjunction with collocated surface magnetic field measurements using a proton precession magnetometer (PPM), provide an insight into the effect of modified tidal components over the equatorial MLT region. In the present study the observed variability in the EEJ, as seen in the EEJ-produced magnetic field at the surface in the form of its “time of peak intensity” and “duration” vis-à-vis the mesopause temperature variation during January–May 2005 is investigated. It is found that a significant part of this variability is a consequence of the presence of a PW of quasi 16 day period and its interactions with the tidal (diurnal and semidiurnal) components.

## 2. Experiments

[6] The unique Multiwavelength Dayglow Photometer [Sridharan *et al.*, 1998] is being operated from Trivandrum

(8.5°N, 77°E; dip latitude, 0.5°N) and can measure intensities of three dayglow emissions (630.0, 731.6, and 740.2 nm) nearly simultaneously [Vineeth *et al.*, 2005, and references therein]. As in the past the daytime OH emission intensity measurements thus obtained were used to estimate the daytime mesopause temperature following the method of Meriwether [1975, 1984]. The measurements at every 10 s interval typically span ~8–10 h during daytime between 0800 and 1800 h for the zenith sky everyday. The temperature data are then averaged for the whole day, and these daylight mean values for the period January–May 2005 are presented in this study. It must be mentioned that the height of the daytime OH layer was inferred to be located at about 90 km over Trivandrum [Kumar *et al.*, 2008] and the temperature measured can be considered to be of that height. The EEJ strength and other parameters are estimated by subtracting the magnetic field measurements of an off-equatorial station (Alibag) from that of the equatorial station (Trivandrum). Hence, the duration of the EEJ (the full width at half-maximum of the daytime EEJ-produced surface magnetic field temporal profile; hereafter,  $D_{EEJ}$ ) and the time of maximum EEJ intensity ( $T_{EEJ}$ ) were estimated. Since the site of the measurements is located right over the magnetic dip equator, the variation in the ground magnetic field essentially represents the horizontal component and is a measure of the EEJ. Days that are geomagnetically severely disturbed ( $A_p > 30$ ), which do not exhibit the typical EEJ-associated daytime  $\Delta H$  variation, are excluded from the analysis. A total of 16 days (days 2, 7, 8, 17, 18, 19, 20, 21, 39, 65, 66, 50, 128, 135, 136 and 150) have been excluded from the analysis because of geomagnetic disturbances. The zonal wind (ZW) and the amplitude and phase of the tidal components at mesospheric altitudes are obtained from collocated SKiYMET (all SKy interferometric METeor) meteor wind radar. The details of this radar have been described elsewhere [Hocking *et al.*, 2004].

## 3. Observations

[7] Figure 1a depicts the day-to-day variation of the mesopause temperature (MT), time of the maximum EEJ ( $T_{EEJ}$ ), and duration of the EEJ ( $D_{EEJ}$ ), over Trivandrum (8.5°N, 76.5°E, 0.5°N dip latitude) for the period January–May 2005. To represent the geomagnetic activity during this period,  $A_p$  indexes are also shown in Figure 1b. During this period significant day-to-day variability is observed in  $T_{EEJ}$  and  $D_{EEJ}$ . On the whole, the mesopause temperature varied between 180 and 215 K during this period. There were prominent increases by ~20 and ~15 K, respectively, around days 40 and 60 and a broad minimum around the spring equinox, i.e., 21 March (day 80). In addition, the temperature exhibited large oscillations up to day 80. Further, it is clear that the  $T_{EEJ}$ ,  $D_{EEJ}$ , and MT appear to be better correlated up to day 80. The time of the  $T_{EEJ}$  showed a shift toward evening, with the  $D_{EEJ}$  becoming large when the MT increased. The observed  $T_{EEJ}$  and  $D_{EEJ}$  trends were opposite when the MT decreased. Apart from this, all the parameters exhibited large-scale oscillations (>10 days) more prominently up to day 80. Apart from the aforementioned parameters, Figure 1b shows one more plot, indicated by quasi 16 day. The origin and relevance of this plot are described in the following paragraph.

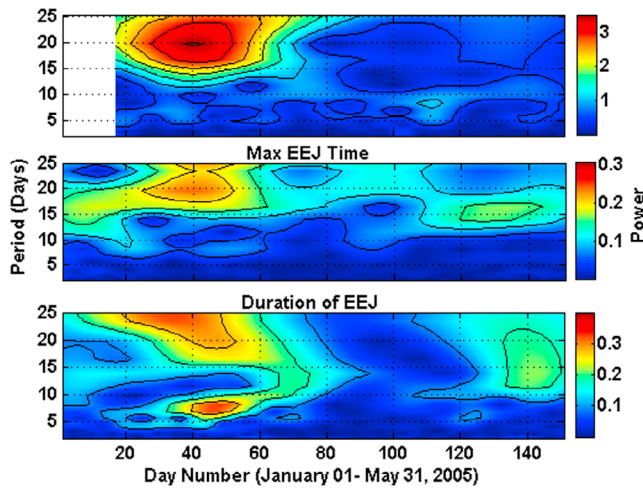


**Figure 2.** Wavelet periodogram for MT,  $D_{EEJ}$ , and  $T_{EEJ}$ .

[8] To determine the nature of the oscillations, a Morlet wavelet analysis [Torrence and Compo, 1998] was performed for each time series, and the results are depicted in Figure 2 as a periodogram. It is clear from Figure 2 that all the parameters show a dominant quasi 16 day periodicity and high wave amplitudes up to day 80. After that, a significant damping of the amplitudes is observed. It must be mentioned that the presence of high wave amplitudes seems to be nearly simultaneous in all the discussed parameters, i.e., MT,  $T_{EEJ}$ , and  $D_{EEJ}$ . The normalized amplitude of the dominant period, i.e., quasi 16 days, is obtained from the wavelet power spectrum of the MT and, as mentioned earlier, is shown in Figure 1 (dashed line) to highlight the possible role of this wave in causing the observed variability in the MT and EEJ parameters. As shown in Figure 1, when the wave executed its positive excursion, the MT exhibited an increase,  $T_{EEJ}$  showed a shift toward evening, and  $D_{EEJ}$  displayed an increase. This correlation between the MT,  $T_{EEJ}$ , and  $D_{EEJ}$  variability continues up to day 80, i.e., during the period when the wave exhibited high amplitudes.

[9] The correlation between the MT and the  $T_{EEJ}$  up to day 80 is found to be  $\sim 0.74$  (correlation coefficient) as shown in Figure 3a, while the overall correlation coefficient (i.e., up to day 151) is only 0.59. In this context the observed correlation coefficient of 0.74 is remarkable, especially since the parameters discussed are totally independent, with the MT being neutral and the others are electrodynamic in nature and represent different altitudinal regions. It must be mentioned here that a similar correlation (correlation coefficient = 0.70) is also seen between the MT and the  $D_{EEJ}$  as shown in Figure 3b. In contrast, no significant correlations (correlation coefficients = 0.15 and 0.19; <30% significance) are found among MT,  $T_{EEJ}$ , and  $D_{EEJ}$  after day 80.

[10] Figure 4 depicts the temporal variation of the amplitude and time of maximum of the diurnal (Figure 4a) and semidiurnal tides (Figure 4b) in the ZW at an altitude of 88 km. To obtain the day-to-day variation of the tidal amplitudes and phases at mesopause altitudes, hourly ZW data at 88 km measured using the collocated meteor wind radar were used. A 4 day moving template was used for this purpose. The first 4 days of observations was used to con-

struct the composite diurnal variation of the ZW. This composite diurnal variation was then subjected to Fourier analysis to obtain the amplitudes and phases of the diurnal and semidiurnal tidal components. These amplitudes and phases were attributed to the first day, and the 4 day template was advanced by 1 day. Perhaps this is the usual procedure followed by many researchers to obtain the day-to-day variations of diurnal and semidiurnal tides [Malinga and Poole, 2002].

[11] It is clear from Figure 4 that both the amplitude and the time of maximum of the diurnal tide exhibited a variability similar to that in MT,  $T_{EEJ}$ , and  $D_{EEJ}$ . The semidiurnal tide also showed large variations in its amplitude and time of maximum, although they were not as prominent as those in the diurnal tide (the amplitude of the diurnal tide is almost two times that of the semidiurnal tide). In addition to these, the amplitude and the time of maximum of both the tidal components showed oscillations of large periodicity (>10 days). The wavelet periodogram as depicted in Figures 5a and 5b reveals the presence of quasi 16 day periodicity up to day 80, corroborating what is shown in Figures 2a–2c. Further, it is clear from Figure 5 that the power of the quasi 16 day wave in the amplitude of the diurnal tide is almost 2 times higher than that for the semidiurnal tide before day 80.

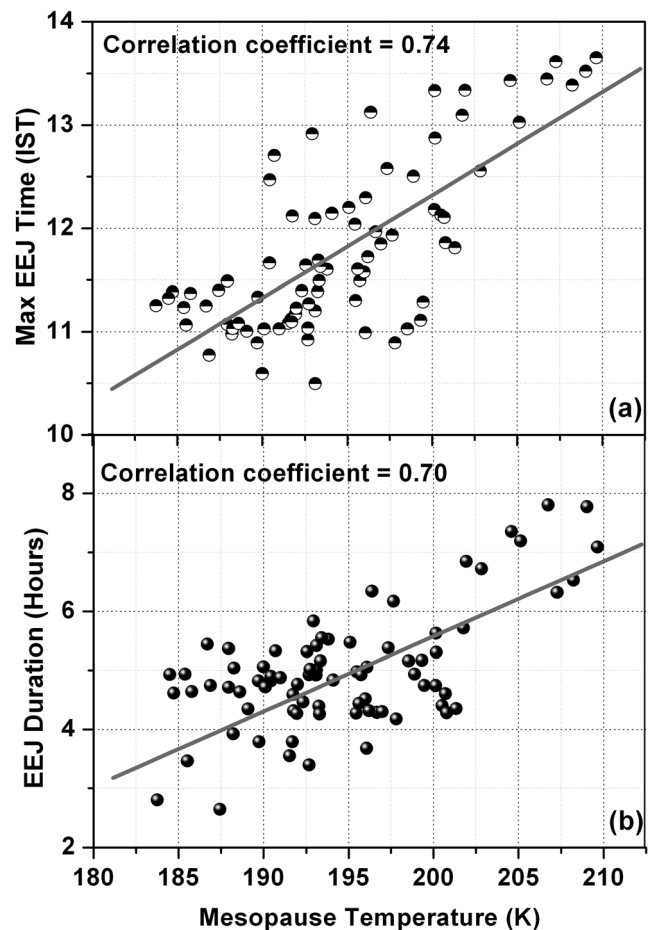


**Figure 3.** Correlation (a) between MT and  $T_{EEJ}$  up to day 80 and (b) between MT and  $D_{EEJ}$  up to day 80. Correlation coefficients shown are above the 95% significance level.

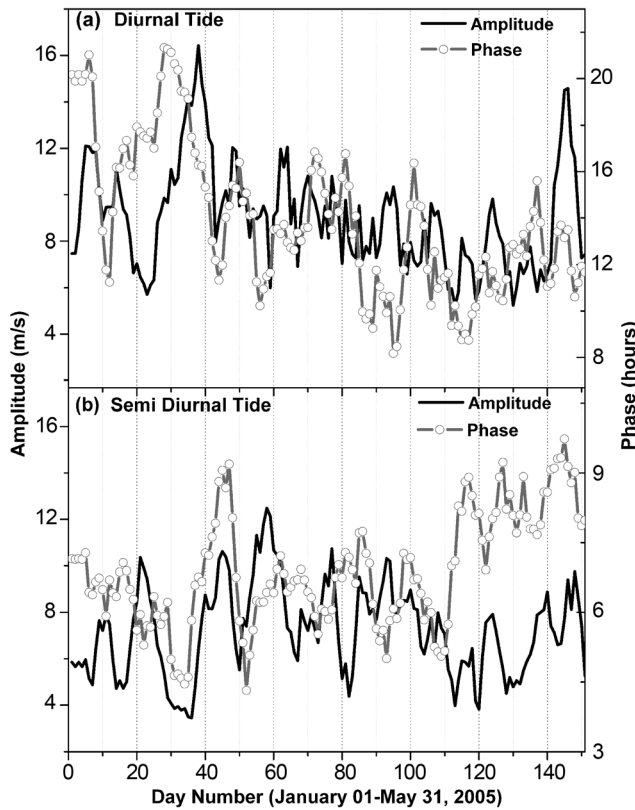


**Figure 4.** Time variation of the amplitude and phase of (a) diurnal and (b) semidiurnal tides in the zonal wind at 88 km.

[12] Figure 6 depicts the daylight mean ZW at 88 km, measured using the meteor wind radar. The neutral wind showed great variability during this period. The wind remained more or less eastward up to day 50. Later it gradually turned westward around day 70. Further, it underwent large oscillations during the early phase of the study, i.e., up to day 70. It is clear from Figure 6 that all the parameters, i.e.,  $T_{EEJ}$ ,  $D_{EEJ}$ , and the tidal components, show large-scale oscillations during the period when the ZW executes its eastward phase. It must be mentioned that after day 140, when the wind turns eastward, the positive correlations exhibited between the discussed parameters become significant once again. Overall, these observations indicate the role that background wind plays in causing changes in the propagation of PWs into the MLT region, which in turn can modulate the mesopause energetics and electrojet parameters over the dip equator.

**4. Results and Discussion**

[13] It is known that upward-propagating tides play a major role in the energetics and dynamics of the equatorial MLT region [Hagan et al., 1999]. The migrating diurnal tide is an important oscillation in the equatorial region that is generated predominantly in the troposphere and propagates vertically to the lower thermosphere, where it grows in amplitude and starts dominating the large-scale wind and temperature fields. Observations have revealed that the amplitude of the tides in the MLT region does not remain

constant over the course of a year but, rather, exhibits a strong semiannual variation, characterized by equinoctial maxima and solstitial minima [Vincent et al., 1998]. Many ground- and satellite-based studies in the past have indicated that the tidal components in the equatorial and low-latitude MLT region undergo large variations as a function of time, height, latitude, and longitude [McLandress et al., 1996; Vincent et al., 1998, and references therein].

[14] Over the dip equator, upward-propagating tides lead to the generation of a global electric field and also the EEJ through the E-region dynamo. Recent studies have shown that upward-propagating tides modulate the E-region electric field and hence the equatorial plasma fountain over the dip equator [Abdu et al., 2006; Immel et al., 2006]. Therefore it can be conjectured that the day-to-day variability in unique equatorial phenomena such as the EEJ is directly connected with the variability in upward-propagating tides.

[15] In contrast, the tides themselves are also known to be modulated by different kinds of waves. It has been shown

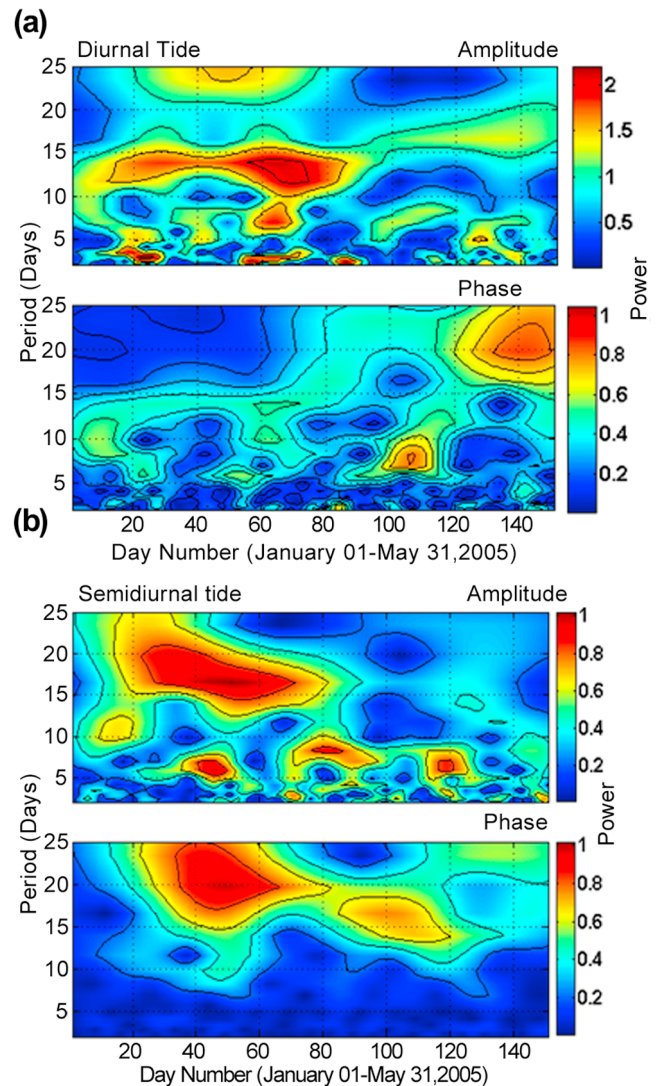


**Figure 5.** Wavelet periodogram for the amplitude and phase of (a) diurnal and (b) semidiurnal tides depicted in Figure 4.

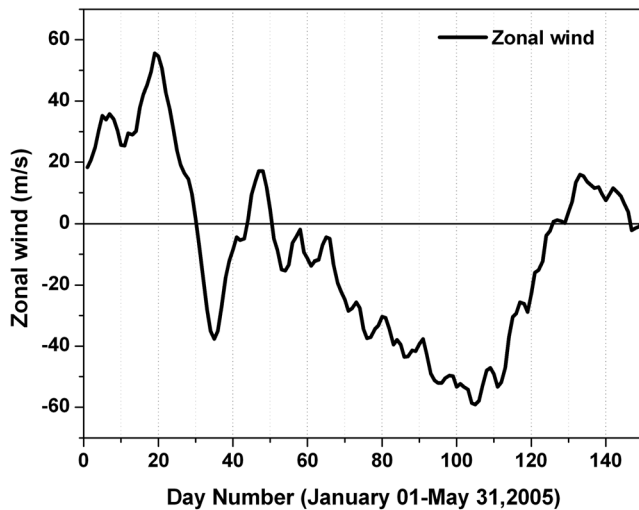


**Figure 6.** Day-to-day variation of daylight mean zonal wind at 88 km.

that the interaction of tides with these waves modifies the amplitude of the tides significantly and also advances their phase [Hagan, 2000]. Some earlier studies have shown that the background wind reveals periodicities of 2–20 days in the 80–100 km regime [Manson and Meek, 1990; Williams and Avery, 1992; Miyoshi, 1999]. Recent studies have revealed that PWs at mesospheric heights are capable of interacting nonlinearly with the tides, modifying the tidal components significantly [Teitelbaum and Vial, 1991; Beard *et al.*, 1999; Mitchell *et al.*, 1999, and references therein]. As mentioned earlier the temperature variability due to the modified tides at upper mesospheric altitude over the equator can be as great as  $\sim 20$  K [Hagan *et al.*, 1999]. In this context the observed oscillations of  $\sim 18$  K in the MT during the period considered in the present study could be easily accounted for.

[16] When it comes to the strong influence of PWs extending up to ionospheric heights, there are two possible mechanisms: (1) PWs originating lower below influencing the generation of electric fields via the modulation of tidal fluxes and (2) a similar influence arising from PWs excited in situ at *E*-region heights by the deposition of gravity wave momentum flux, which itself is modulated by PW interaction at lower heights [Forbes *et al.*, 1995]. The first mechanism seems promising, in view of the fact that the upward-propagating diurnal components are basically responsible for the unique processes in the quiet-time ionosphere, especially over equatorial latitudes. In fact, analysis of ionospheric data in the past has revealed the presence of a quasi 16 day oscillation consistent with the 16 day modulation of *E*-region dynamo winds of the order of  $10 \text{ ms}^{-1}$  [Forbes and Leveroni, 1992].

[17] An explanation for the presence of PWs in the EEJ was given by Abdu *et al.* [2006] in a recent study. The EEJ-produced magnetic field represents the diurnal variation in the EEJ, which is a direct measure of the product of dynamo electric field intensity, electron density and conductivity at *E*-region heights. Since there is no direct evidence for PW oscillation in *E*-region electron density, which is dependent solely on the solar zenith angle on a given day, the variation

in EEJ intensity could be attributed to the oscillation in the dynamo electric field produced by the tidal winds. Further, since it is the product of the conductivity, electron density and the strength of the tidal wind that determines the EEJ structure on a given day, the phase change in the tides would significantly affect the duration, strength, and time of maximum of the EEJ. So the observed changes in EEJ parameters could be attributed to changes in the tidal structure. It is evident from Figures 5 and 6 that the tidal components are indeed modulated by the quasi 16 day wave, which is more prominent up to day 80, accounting for the variability seen in the EEJ parameters in the present study. In fact it is seen that when the quasi 16 day wave executes its positive excursion, the diurnal tide appears to advance toward afternoon, and during the wave's negative excursion, the tide undergoes a phase shift toward morning (Figures 4a and 4b). After day 80 the quasi 16 day wave shows significant damping, and its correlations with other parameters become poor. As mentioned earlier, a similar relationship is seen among MT,  $T_{EEJ}$ , and  $D_{EEJ}$ , clearly indicating the role of tides modulated by the PWs therein.

[18] The electron density and conductivity, which are solely dependent on solar zenith angle, are not expected to change from one day to another during quiet solar conditions. In a given epoch the time of the peak EEJ will be directly tied to the phase of the diurnal tide. When the time of maximum production of electron density and the positive phase of the diurnal tide coincide, the EEJ will become more intense, with an increased half-intensity duration. The shift toward afternoon of the time of the peak EEJ observed on days 40 and 60 and the subsequent broadening in the duration of the EEJ confirm this aspect. Although the amplitude of the diurnal tide is found to be almost 2 times higher than that of the semidiurnal tide, it is not possible to exclude the role of the semidiurnal tide in modulating the parameters discussed. Similarly, the periodicity seen in the diurnal tide is  $\sim 13$  days and the semidiurnal component is  $\sim 20$  days. This disparity is believed to be due to the differences in interaction between the PW and the tidal components. The nature of interaction might be totally different for diurnal and semidiurnal tidal components. However, the exact reason for this difference is not known at the moment. Nevertheless, both of these components play a combined role in modulating the EEJ components, and at present it is difficult to delineate their contribution. Further, the observed time shift between these parameters on some of the days, like days 50 and 65, cannot be explained by PW-tidal interactions alone. However, as explained by Ortland [2005], the presence of gravity waves can also change the vertical wavelength and shift the phase of the tides. It is known that gravity waves may exhibit significant day-to-day variability. In this context, the observed time shifts on days 50 and 65 could be ascribed to the change in the upward-propagating gravity wave fluxes. However, the present database is not sufficient to address and quantify this aspect.

[19] Nonetheless, the long-period PWs are shown to be incapable of penetrating to mesopause heights from their lower-atmosphere source regions through the westward winds of the summer stratosphere and mesosphere [Charney and Drazin, 1961]. For long-period PWs ( $>10$  days) with low westward phase velocities, propagation into the westward

regime is precluded. *Espy et al.* [1997] attributed this observation to the blocking of the wave's propagation from the winter hemisphere during the westward phase of the equatorial quasi-biennial oscillation in the upper stratosphere. This explains the damping observed in the quasi 16 day wave after day 70, where the ZW shows a sharp westward excursion. However, it must be mentioned that the tides would contribute to the daylight mean ZW, and this would indeed have an effect on the propagation or blocking of the PWs mentioned. Overall, in the low-latitude MLT region the effects of PW-tidal interactions are expected to be maximum at an altitude of between 70 and 120 km, i.e., where the amplitude of the diurnal tide is maximum. Further, the effect would be nearly simultaneous in the mesopause (~90 km) and the EEJ (~105 km) region because of the large vertical wavelength of the diurnal tide (~35 km).

## 5. Conclusion

[20] The implications of wave-tidal interactions for the equatorial MLT region are discussed. The PW is found to modulate the daytime MT and the duration and time of maximum of the EEJ. The wave-tidal interaction and the subsequent modification of the tidal components are found to be the reason for this nearly simultaneous wave amplification. Although many MLT parameters are known to show PW amplification during winter months over other latitudes, the present findings, showing the effect of a quasi 16 day wave on "dip equatorial" energetics, dynamics, and electrodynamics simultaneously, are new and have great implications for the MLT coupling.

[21] **Acknowledgments.** This work was supported by the Department of Space, Government of India. C. Vineeth gratefully acknowledges the financial assistance provided by the Indian Space Research Organization.

[22] Robert Lysak thanks the reviewers for their assistance in evaluating this paper.

## References

- Abdu, M. A., et al. (2006), Planetary wave signatures in the equatorial atmosphere-ionosphere system, and mesosphere-E- and F-region coupling, *J. Atmos. Sol. Terr. Phys.*, *68*, 509–522.
- Beard, A. G., et al. (1999), Non-linear interactions between tides and planetary waves resulting in periodic tidal variability, *J. Atmos. Sol. Terr. Phys.*, *61*, 363–376.
- Charney, J. G., and P. G. Drazin (1961), Propagation of planetary-scale disturbances from the lower into the upper atmosphere, *J. Geophys. Res.*, *66*, 83–109.
- Deepa, V., G. Ramkumar, M. Antonita, K. K. Kumar, and M. N. Sasi (2006), Vertical propagation characteristics and seasonal variability of tidal wind oscillations in the MLT region over Trivandrum (8.5°N, 77°E): First results from SKiYMET meteor radar, *Ann. Geophys.*, *24*, 2887–2889.
- Espy, P. J., J. Stregmann, and G. Witt (1997), Interannual variation of the quasi-16-day oscillation in the polar summer mesospheric temperature, *J. Geophys. Res.*, *102*, 1983–1990, doi:10.1029/96JD02717.
- Fambitakoye, O., and P. N. Mauyau (1976), Equatorial electrojet and regular daily variation  $S_R$ : I. A determination of electrojet parameters, *J. Atmos. Sol. Terr. Phys.*, *38*, 1–17.
- Forbes, J. M. (1981), Equatorial electrojet, *Rev. Geophys.*, *19*, 469–504.
- Forbes, J. M., and S. Leveroni (1992), Quasi 16-day oscillations in the ionosphere, *Geophys. Res. Lett.*, *19*, 981–984.
- Forbes, J. M., M. E. Hagan, S. Miyahara, F. Vial, A. H. Manson, C. E. Meek, and Y. I. Portnyagin (1995), Quasi 16-day oscillation in the mesosphere and lower thermosphere, *J. Geophys. Res.*, *100*, 9149–9163.
- Hagan, M. E. (2000), Atmospheric tidal propagation across the stratopause, in *Atmospheric Science Across the Stratopause*, *Geophys. Monogr. Ser.*, vol. 123, edited by D. E. Siskind, S. D. Eckermann, and M. E. Summers, pp. 177–190, AGU, Washington, D. C.
- Hagan, M. E., M. D. Burrage, J. M. Forbes, J. Hackney, W. J. Randel, and X. Zhang (1999), GSWM-98: Results for migrating solar tides, *J. Geophys. Res.*, *104*, 6813–6828.
- Hocking, W. K., W. Singer, J. Bremer, M. J. Mitchell, P. Batista, B. Clemesha, and M. Donner (2004), Meteor radar temperatures at multiple sites derived with SKiYMET radars and compared to OH, rocket, and Lidar measurements, *J. Atmos. Sol. Terr. Phys.*, *66*, 585–593.
- Immel, T. J., E. Sagawa, S. L. England, S. B. Henderson, M. E. Hagan, S. B. Mende, H. U. Frey, C. M. Swenson, and L. J. Paxton (2006), Control of equatorial ionosphere morphology by atmospheric tides, *Geophys. Res. Lett.*, *33*, L15108, doi:10.1029/2006GL026161.
- Kumar, K. K., C. Vineeth, T. M. Antonita, T. K. Pant, and R. Sridharan (2008), Determination of day-time OH emission heights using simultaneous meteor radar, day-glow photometer and TIMED/SABER observations over Thumba (8.5°N, 77°E), *Geophys. Res. Lett.*, *35*, L18809, doi:10.1029/2008GL035376.
- Malinga, S. B., and M. G. Poole (2002), The 16-day variation in tidal amplitudes at Grahamstown (33.3°S, 26.5°E), *Ann. Geophys.*, *20*, 2033–2038.
- Manson, A. H., and C. E. Meek (1990), Long period (~8–20 h) wind oscillations in the upper middle atmosphere at Saskatoon (52°N): Evidence for non-linear tidal effects, *Planet. Space Sci.*, *38*, 1431–1441.
- McLandress, C., G. G. Shepherd, and B. H. Solheim (1996), Satellite observations of thermospheric tides: Results from the Wind Imaging Interferometer on UARS, *J. Geophys. Res.*, *101*, 4093–4114.
- Meriwether, J. W. (1975), High latitude airglow observations of correlated short-term fluctuations in the hydroxyl Meinel 8–3 band intensity and rotational temperature, *Planet. Space Sci.*, *23*, 1211–1221.
- Meriwether, J. W. (1984), Ground based measurements of mesospheric temperatures by optical means, *MAP Handb.*, *13*, 1–18.
- Mitchell, N. J., et al. (1999), The 16-day planetary wave in the mesosphere and lower thermosphere, *Ann. Geophys.*, *17*, 1447–1456.
- Miyoshi, Y. (1999), Numerical simulation of the 5-day and 16-day waves in the mesopause region, *Earth Planets Space*, *51*, 763–772.
- Ortland, D. A. (2005), A study of the global structure of the migrating diurnal tide using generalized Hough modes, *J. Atmos. Sci.*, *62*, 2684–2702.
- Reddy, C. A. (1981), The equatorial electrojet: A review of the ionospheric and geomagnetic aspects, *J. Atmos. Terr. Phys.*, *43*, 557–571.
- Reddy, C. A. (1989), The equatorial electrojet, *Pure Appl. Geophys.*, *131*, 485–508.
- Richmond, A. D. (1973), Equatorial electrojet: I. Development of a model including winds and instabilities, *J. Atmos. Terr. Phys.*, *66*, 1083–1103.
- Smith, A. K. (2004), Physics and chemistry of the mesopause region, *J. Atmos. Sol. Terr. Phys.*, *66*, 839–857.
- Sridharan, R., N. K. Modi, D. Pallam Raju, R. Narayanan, T. K. Pant, A. Taori, and D. Chakrabaty (1998), Multiwavelength daytime photometer—a new tool for the investigation of atmospheric processes, *Meas. Sci. Technol.*, *9*, 585–591, doi:10.1088/0957-0233/9/4/005.
- Stening, R. J. (1985), Modelling the equatorial electrojet, *J. Geophys. Res.*, *90*, 1705–1715.
- Teitelbaum, H., and F. Vial (1991), On tidal variability induced by nonlinear interaction with planetary waves, *J. Geophys. Res.*, *96*, 169–178.
- Torrence, C., and G. P. Compo (1998), A practical guide to wavelet analysis, *Bull. Am. Meteorol. Soc.*, *79*, 61–78.
- Vincent, R. A., S. Kovalam, D. C. Fritts, and J. R. Isler (1998) Long-term MF radar observations of solar tides in the low-latitude mesosphere: Interannual variability and comparisons with the GSWM, *J. Geophys. Res.*, *103*, 8667–8883.
- Vineeth, C., T. K. Pant, M. Antonita, G. Ramkumar, C. V. Devasia, and R. Sridharan (2005), A comparative study of daytime mesopause temperatures obtained using unique ground-based optical and meteor wind radar techniques over the magnetic equator, *Geophys. Res. Lett.*, *32*, L19101, doi:10.1029/2005GL023728.
- Vineeth, C., T. K. Pant, C. V. Devasia, and R. Sridharan (2007), Atmosphere-ionosphere coupling observed over the dip equatorial MLT region through the quasi 16-day wave, *Geophys. Res. Lett.*, *34*, L12102, doi:10.1029/2007GL030010.
- Williams, C. R., and S. K. Avery (1992), Analysis of long-period waves using the mesosphere-stratosphere-troposphere radar at Poker Flat, Alaska, *J. Geophys. Res.*, *97*, 20,855–20,861.

S. Gurubaran, Equatorial Geophysical Research Laboratory, Krishnapuram, Tirunelveli 627011, India.

K. K. Kumar, T. K. Pant, S. G. Sumod, and C. Vineeth, Space Physics Laboratory, Vikram Sarabhai Space Centre, 695022 Trivandrum, India. (cnvins@gmail.com)

R. Sridharan, Physical Research Laboratory, Navarangapura, Ahmedabad 380009, India.